Japanese Journal of Applied Physics
Vol. 46, No. 4A, 2007, pp. 1656–1662

Theoretical Interpretation of Anomalous Enhancement of Nuclear Reaction Rates Observed at Low Energies with Metal Targets

Yeong E. KIM* and Alexander L. ZUBAREV†

Purdue Nuclear and Many-Body Theory Group (PNMBTG), Department of Physics, Purdue University, West Lafayette, IN 47907, U.S.A.

(Received October 17, 2006; revised December 22, 2006; accepted January 30, 2007; published online April 5, 2007)

A theoretical interpretation is presented for anomalous enhancements of nuclear reaction rates for deuteron–deuteron, deuteron–lithium, and proton–lithium reactions that were recently observed at low energies from deuteron and proton beam experiments. Using a generalized momentum-distribution function derived by Galitskii and Yakimets, which has high-energy momentum distribution tail of the inverse eighth power of the momentum, we obtain an approximate semi-analytical formula for nuclear reaction rates. Comparison of our theoretical estimates with recent experimental data indicates that the theory may provide a reasonable and consistent theoretical explanation of the experimental data. Based on predictions of our theoretical formula, we suggest a set of experiments for testing some of the theoretical predictions. [DOI: 10.1143/JJAP.46.1656]

KEYWORDS: nuclear reactions involving few-nucleon systems, quantum statistical mechanics, energy loss and stopping power, few-body systems, and particle measurements

1. Introduction

In 1988, an anomalous enhancement of the low-energy fusion cross-section was observed by Engstler *et al.* for the reaction ^{3}He(d,p)^{4}He,[1] and then in 1995 by Greipe *et al.* for (D+D) fusion.[2] Experimental probes of low-energy nuclear reactions in metals with deuteron beams were first suggested in 1995 by Kasagi *et al.*[3] Anomalously large values of electron screening energies, U_e, were observed by Yuki *et al.*[4,5] with ytterbium (Yb) target[4] in 1997, and with palladium (Pd) and palladium oxide (PdO) targets[5] in 1998. Since then, there have been many experimental observations of anomalous values of U_e with other metal targets,[6–14] which have much larger values than atomic electron screening potential energies, U_A.[15,16]

Many physical models have been considered to explain these anomalies without success (see ref. 8 for a list). Recently an electron plasma model of Debye–Hückel in metals was proposed as a possible explanation of the large effects in metals by Raiola *et al.*[11,13,17] They have applied this classical plasma electron screening model of Debye to quasi-free metallic electrons, and claimed some successes in co-relating the observed values of U_e including its temperature dependence. However, this agreement may turn out to be fortuitous, since the condition $e\phi(r) < kT$ is not satisfied for their case. The potential $\phi(r) = Ze\exp(-r/R_D)/r$ with $R_D = [kT/4\pi n_0 e^2]^{1/2}$, valid only for $e\phi < kT$, is a solution of the Poisson equation for a test charge Ze placed at the origin in a distribution of electrons (charge density, $-en_0$) with its uniform background of positive ions.[18] For their case of $e\phi(R_D) > kT$, the corresponding Poisson equation for $\phi(r)$ is a non-linear equation for which we do not know its solution at present. Furthermore, the classical plasma theory of Debye is valid only if there are enough particles (electrons) in the cloud, $N_D \gg 1$, where $N_D = (4\pi/3)n_0 R_D^3$. For the above case, $N_D \approx 3 \times 10^{-5}$, and hence the Debye theory may not be applicable for this case as pointed out by Coraddu *et al.*[19]

More recently Coraddu *et al.*[19–21] used a modified momentum distribution introduced by Galitskii and Yakimets,[22] in an attempt to explain the anomalies. As shown by Galitskii and Yakimets (GY)[22] the quantum energy indeterminacy due to interactions between particles in a plasma leads to a generalized momentum distribution which has a high-energy momentum distribution tail diminishing as an inverse eighth power of the momentum, instead of the conventional Maxwell–Boltzmann distribution tail which decays exponentially. GY's generalized momentum distribution has been used by Coraddu *et al.*[19–21] for deuterons in a metal target in an analysis of anomalous cross-sections for D(d,p)^{3}H observed from the low-energy deuteron beam experiments.[8,9,11] Their calculated results for the fusion rates between the beam deuteron and quasi-free mobile deuteron in a metal target are too small to explain the observed experimental anomalies.[6,7,9] Most recently, however, we have investigated and found that the effect of the GY distribution on nuclear fusion rates in plasma is significantly large for (D+D) reactions, and also for (D+Li) and (p+Li) reactions.[23] In ref. 23, this type of nuclear fusion process due to the quantum correction of the conventional momentum distribution function was named as "quantum plasma nuclear fusion" (QPNF).

In this paper, we investigate the effect of the QPNF for anomalous results observed in the beam experiments with metal targets. The calculated results for deuteron–deuteron (D+D) fusion rates are compared with the experimental results.[8,9,11] In addition, we investigate other nuclear fusion rates for (D+Li)[10] and (p+Li)[14] reactions in metal targets at low energies.

2. Physical Model for Low-Energy Deuteron (Proton) Beam Experiments with Metal Targets

Recent results of cross-section measurements from deuteron beam experiments with metal targets by Kasagi *et al.*[7,10] and Raiola *et al.*[8,9,11] indicate that anomalous enhancement of nuclear reaction cross-sections at low energies occurs mostly with metal targets.

Recently, Raiola *et al.*[11] have investigated the electron screening effect in the D(d,p)^{3}H reaction with a low energy (center-of-mass energies between ~ 2 and ~ 15 keV) deuteron beam on deuterated targets (32 metals, 4 insulators, 3 semiconductors, 6 groups 3, 4 elements, and 13 lanthanides). They have found that nearly all deuterated metals yield large

*E-mail address: yekim@physics.purdue.edu
†E-mail address: zubareva@physics.purdue.edu

extracted values of the screening energy U_e ranging from $U_e = 180 \pm 40\,\text{eV}$ (Be) to $U_e = 800 \pm 90\,\text{eV}$ (Pd), while all deuterated non-metal targets yield smaller values of $U_e \leq 80\,\text{eV}$.

2.1 Reaction zone

For a metal target, we define a reaction zone where nuclear reactions take place. For the incoming particle beam (proton or deuteron) with the beam diameter D_b, the volume of the reaction zone is defined as

$$V_{\text{int}}(E_i) = A\Delta x(E_i) \tag{1}$$

where $A = \pi D_b^2/4$ and $\Delta x(E_i)$ is the range of the beam particles with the laboratory energy E_i. The beam diameters and beam currents, (D_b, I_B), used for the experiments are ($\sim$15 mm, $\sim$60 μA), ($\sim$4 mm, $\sim$100 μA), and ($\sim$10 mm, $\lesssim$20 μA), respectively for D+D,[8] D+Li,[10] and p+Li[14] reactions. $\Delta x(E_i)$ is given by[16]

$$\Delta x(E_i) = \int dx = \int_0^{E_i} \left(\frac{dE}{dx}\right)^{-1} dE \tag{1b}$$

where (dE/dx) is the stopping power.[24] For a proton laboratory kinetic energy of $1 \leq E \lesssim 10\,\text{keV}$, it is given by

$$\frac{dE}{dx} = A_1 n^t E^{1/2} \times 10^{-18}\,\text{keV}\cdot\text{cm}^2 \tag{2}$$

where n^t is the number density of the target atom in units of cm^{-3}, and the coefficient A_1 is given in ref. 24.

For a proton kinetic energy of $10\,\text{keV} \leq E \leq 1\,\text{MeV}$, we have

$$\left[\frac{dE}{dx}\right]^{-1} = \left[\frac{dE}{dx}\right]_{\text{slow}}^{-1} + \left[\frac{dE}{dx}\right]_{\text{high}}^{-1}, \tag{3}$$

where

$$\left[\frac{dE}{dx}\right]_{\text{slow}} = n^t A_2(E)^{0.45} \times 10^{-18}\,\text{keV}\cdot\text{cm}^2, \tag{3a}$$

and

$$\left[\frac{dE}{dx}\right]_{\text{high}} = (n^t A_3/E)\ln[1 + A_4/E + A_5 E] \times 10^{-18}\,\text{keV}\cdot\text{cm}^2 \tag{3b}$$

The coefficients A_i ($i = 2-5$) are given in ref. 24. For a deuteron laboratory kinetic energy E, dE/dx is obtained by replacing E by $E/2$ in eqs. (2), (3), (3a), and (3b).

2.2 Mobility of hydrogen and deuterium in metals

Hydrogen (or deuterium) molecules in Palladium are known to be dissociated into atoms and ionized to bare nuclei.[25] This may be occurring for other metals. The mobility of protons and deuterons in Pd and other metals has been experimentally demonstrated, in particular under applied currents.[26,27] However, other heavier nuclei (Li, B, etc.) are most likely to have much less mobility and most of them may be stationary in metal/alloy lattices.

More recent kinematic measurements for the D(d,p)T reaction in metal targets with the deuteron beam with deuteron energies $\sim$10–20 keV indicate that deuterons in the metal target are mobile.[28] The extracted values of deuteron effective kinetic energies 50, 150, and 300 eV[28] in the metal targets Au, Pd, and PdO, respectively, cannot be explained by the conventional Maxwell–Boltzmann distribution of deuterons at the near ambient temperatures.

For our physical model, it is assumed as in refs. 23 and 29 that, although most of the deuterons (or protons) in a metal target are in localized states, a very small fraction of them is in a quasi-free mobile plasma state[30] within the reaction zone volume and attains a generalized momentum distribution of the GY type during the steady state achieved with incoming deuteron (or proton) beam.

2.3 Quantum corrections to particle-momentum distributions

The distribution functions f(p) at large momentum p for dilute gases at $T = 0$ are given by $f(\boldsymbol{p}) = (\hbar a^2/2\pi)\rho/p^4$ for spin 1/2; fermions[31,32] and $f(\boldsymbol{p}) = \hbar(2\pi a^2/\pi^2)\rho/p^4$ for bosons,[33,34] where a is the scattering length and ρ is the number density. We note that the total cross-section for the hard-core interaction is $\sigma = 2\pi a^2$. For charged particles at finite temperatures, the generalized distribution function for energy E and momentum p is derived by GY[22] is given as

$$f(E, \boldsymbol{p}) = n(E)\delta_\gamma(E, \varepsilon_p) \tag{4}$$

where $n(E)$ is the occupation number. $\delta_\gamma(E, \varepsilon_p)$ is the spectral function given by

$$\delta_\gamma(E, \varepsilon_p) = \frac{\gamma(E, \boldsymbol{p})}{\pi[(E - \varepsilon_p - \Delta(E, \boldsymbol{p}))^2 + \gamma^2(E, \boldsymbol{p})]} \tag{5}$$

where $\gamma(E, \boldsymbol{p})$ is the width of the momentum-energy dispersion, $\Delta(E, \boldsymbol{p})$ is the energy shift and ε_p is the center of mass kinetic energy, $\varepsilon_p = p^2/2\mu$.

From eq. (4) we obtain the momentum distribution

$$df(\boldsymbol{p}) \approx N_A\left[\int_0^\infty dE\,\delta_\gamma(E, \varepsilon_p)n(E)\right]d^3p. \tag{6}$$

For exact function $\gamma(E, \boldsymbol{p})$ and $\Delta(E, \boldsymbol{p})$, $N_A = 1$, but in the case of approximate γ and Δ, N_A may depend on the temperature.

If we assume that[20]

$$\gamma(E, \varepsilon_p) \approx \hbar\rho_c\sigma_c\sqrt{\frac{2E}{\mu}}, \tag{7}$$

where $\sigma_c = \pi(Z_i^e Z_j^e e^2)^2/\varepsilon_p^2, \varepsilon_p = p^2/2\mu$, ρ_c is the number density, μ is the reduced mass, and $Z_i^e e$ is an effective charge which may depend on ε_p, then we obtain for a high momentum region

$$df(\boldsymbol{p}) \propto N_A\frac{d^3p}{p^8}. \tag{8}$$

This is to be compared with the other conventional cases, $f(\boldsymbol{p}) \propto e^{-\varepsilon_p/kT}$ for Maxwell–Boltzmann (MB), Fermi–Dirac (FD), and Bose–Einstein (BE) distributions. GY theory predicts that N_A is not significantly different from unity.

2.4 Reaction processes occurring in reaction zone

During the steady state achieved with an incoming deuteron (or proton) beam, we consider four possible types of reaction processes:

(1) the incident beam deuteron (or proton) reacts with the stationary deuteron (or Li) in the target, i.e., between

beam particle and target particle (bt);
(2) the incident beam deuteron (or proton) reacts with deuteron (or proton) in the plasma state, i.e., between beam particle and particle in the plasma (bp);
(3) deuterons (or protons) in the plasma state react with each other, i.e., between plasma particles (pp); and
(4) deuteron (or proton) in the plasma state react with stationary deuteron (or Li) in the target, i.e., between plasma particle and target particle (pt).

3. Reaction Rate Formulae Based on Quantum Plasma Nuclear Fusion

We now proceed to calculate the plasma fusion rate R^{Q} using the generalized distribution function $f(p)$ with the tail given by eqs. (6) and (8). R^{Q} is a new quantum correction to the conventional nuclear fusion rate in a plasma. We now derive an approximate analytical formula for QPNF in order to obtain an order-of-magnitude estimate for the nuclear fusion rate.

3.1 Fusion reaction rates

The total nuclear fusion rate, R_{ij}, per unit volume (cm^{-3}) and per unit time (s^{-1}) between a pair of nuclei, i and j is given by

$$R_{ij} = R_{ij}^{\mathrm{bt}} + R_{ij}^{\mathrm{bp}} + R_{ij}^{\mathrm{pp}} + R_{ij}^{\mathrm{pt}} \tag{9}$$

where R_{ij}^{bt}, R_{ij}^{bp}, R_{ij}^{pp}, and R_{ij}^{pt} are nuclear reaction rates between a beam particle and a target particle (bt), a beam particle and a plasma particle (bp), a plasma particle and a plasma particle (pp), and a plasma particle and a target particle (pt), respectively.

R_{ij}^{bt} is given by[16)]

$$R_{ij}^{\mathrm{bt}}(E_0, U_{\mathrm{e}}) = \Phi_i \rho_{\mathrm{t}} \int_0^{E_0} \frac{dE_i}{|dE_i/dx|}\, \sigma_{ij}(E, U_{\mathrm{e}}) \tag{10}$$

where Φ_i is the incident beam particle flux (# per cm^2), ρ_{t} is the stationary target particle density, E_0 is the incident kinetic energy in the laboratory system, $|dE_i/dx|$ is the stopping power[24)] with the laboratory kinetic energy E_i, and $\sigma_{ij}(E)$ is the cross-section for reaction between particles i and j with the relative kinetic energy E in the center of mass (CM) system. $\sigma_{ij}(E)$ is conventionally parameterized as

$$\sigma_{ij}(E) = \frac{S(E)}{E} \exp[-\sqrt{E_{\mathrm{G}}/E}] \tag{11}$$

where E_{G} is the Gamow energy, $E_{\mathrm{G}} = (2\pi\alpha Z_i Z_j)^2 \mu c^2/2$ with the reduced mass μ, and $S(E)$ is the astrophysical S-factor. To accommodate the effect of electron screening for the target nuclei, $\sigma_{ij}(E)$ is modified to include the electron screening energy, U_{e}, and parameterized as

$$\sigma_{ij}(E, U_{\mathrm{e}}) = \frac{S(E + U_{\mathrm{e}})}{E + U_{\mathrm{e}}} \exp[-\sqrt{E_{\mathrm{G}}/(E + U_{\mathrm{e}})}] \tag{12}$$

The other terms in eq. (9), R_{ij}^{bp}, R_{ij}^{pp}, and R_{ij}^{pt}, are reaction rates due to new processes involving the quasi-free mobile deuterons in a plasma state with a momentum distribution of the GY type. R_{ij}^{bp} and R_{0j}^{pp} are expected to be much smaller than R_{ij}^{pt} based on consideration on different densities involved. The recent calculation by Coraddu *et al.*[19)] indicates that R_{ij}^{bp} is negligible.

3.2 Dominant contribution from quantum plasma nuclear fusion

R_{ij}^{pt} can be written as

$$R_{ij}^{\mathrm{pt}} \approx V_{\mathrm{int}}(E_0)(R_{ij}^{\mathrm{C}} + R_{ij}^{\mathrm{Q}}) \tag{13}$$

where $V_{\mathrm{int}}(E_0)$ is given by eq. (1), R_{ij}^{C} is the conventional fusion rate calculated with the MB distribution, and R_{ij}^{Q} is the QPNF contribution which can be calculated using eqs. (4) and (7). It is given by

$$\begin{aligned} R_{ij}^{\mathrm{Q}} &= N_{\mathrm{A}} \frac{\rho_i \rho_j}{1 + \delta_{ij}} \langle \sigma v_{\mathrm{rel}} \rangle \\ &\approx \frac{1}{1 + \delta_{ij}} N_{\mathrm{A}}(4(5!)) \frac{(\hbar c)^3}{\mu c} \alpha^2 S_{ij}(0)(Z_i^{\mathrm{e}} Z_j^{\mathrm{e}})^2 \frac{\rho_{\mathrm{c}} \rho_i \rho_j}{E_{\mathrm{G}}^3} \end{aligned} \tag{14}$$

where E_{G} is the Gamow energy, $E_{\mathrm{G}} = (2\pi\alpha Z_i Z_j)^2 \mu c^2/2$, ρ_i is the number density of nuclei, and $S_{ij}(0)$ is the S-factor at zero energy for a fusion reaction between i and j nuclei. Equation (14) is obtained by assuming $S_{ij}(E) \approx S_{ij}(0)$. In general, both N_{A} and ρ_i may depend on the temperature. For the remainder of this paper, we will set $N_{\mathrm{A}} = 1$. Although the formula, eq. (14), is derived originally for identical particles (one-specie plasma case), it is assumed that the same formula can be generalized and applied to some two-species cases.

Because of the quasi-free deuteron mobility in metals, (D+D) fusion rates in metals were investigated using the MB velocity distribution for deuterons with a hope that the high-energy tail of the MB distribution may increase the (D+D) fusion rates in metals.[39)] However, the calculated results for the (D+D) fusion rates with the MB distribution were found to be extremely small at ambient temperatures.[35)]

R_{ij}^{Q} given by eq. (14) covers three different cases:
(a) Nuclei i and j are the same specie and mobile in a plasma with a generalized velocity distribution (for example, i and j are both deuterons yielding the (D+D) fusion reaction rate).
(b) Nuclei i and j are two different species and both mobile in a mixed two-species plasma with velocity distributions (for example, i is for protons and j is for deuterons yielding the (p+D) fusion reaction).
(c) Nucleus i is mobile and they form a single-specie plasma with a velocity distribution, but nucleus j is stationary and imbedded in a metal/alloy matrix. Nuclei i and j are the same specie (for example, i and j are both protons or both deuterons) or nuclei i and j are two different species yielding (D+Li), (p+Li) or (p+B) fusion reactions.

3.3 Parameterization of experimental data for low-energy reaction rates

For comparison of our theoretical estimates with experimental data, we use the parameterization of the experimental data for anomalous enhancement based on the following equation,

$$R_{ij}^{\mathrm{exp}}(E_0, U_{\mathrm{e}}^{\mathrm{exp}}) \approx \Phi_i \rho_{\mathrm{t}} \int_0^{E_0} \frac{dE_i}{|dE_i/dx|}\, \sigma_{ij}(E, U_{\mathrm{e}}^{\mathrm{exp}}) \tag{15}$$

where $\sigma_{ij}(E, U_{\mathrm{e}}^{\mathrm{exp}})$ is given by eq. (12) with U_{e} replaced by experimentally extracted value of $U_{\mathrm{e}}^{\mathrm{exp}}$ obtained by fitting the experimental data. When $U_{\mathrm{e}}^{\mathrm{exp}}$ turns out to be much larger than the adiabatic value U_{A},[36)] it cannot be theoret-

ically justified. However, eq. (15) with a large value of U_e^{exp} is still useful as a convenient parameterization of the experimental data. R_{ij}^{ext} given by eq. (15) will be compared with theoretical estimates of the reaction rates based on R_{ij} given by eq. (9).

4. Applications to Experimental Results of Low-Energy Nuclear Reactions

For our theoretical estimates for R_{ij}, we approximate it using eq. (13), as

$$R_{ij} \approx R_{ij}^{bt} + R_{ij}^{pt} \approx R_{ij}^{bt} + V_{int}(E_0)R_{ij}^{Q} \tag{16}$$

where R_{ij}^{bt} is given by eq. (10) and R_{ij}^{Q} is given by eq. (14). Comparisons will be made with the experimental data from the (D+D), (p+Li), and (D+Li) reactions.

For comparison between the experimental data and theoretical estimates, we introduce the enhancement factor $F(E)$ defined as

$$F_{exp}(E) = \frac{R_{ij}^{exp}(E, U_e^{exp})}{R_{ij}^{bt}(E, U_A)}, \tag{17}$$

and

$$F_{theo}(E) \approx \frac{R_{ij}^{bt}(E, U_A) + V_{int}(E)R_{ij}^{Q}}{R_{ij}^{bt}(E, U_A)}, \tag{18}$$

where $V_{int}(E)$, $R_{ij}^{bt}(E, U_A)$, R_{ij}^{Q}, and $R_{ij}^{exp}(E, U_e^{exp})$ are given by eqs. (1), (10), (14), and (15), respectively. U_A is the adiabatic value for the screening energy, $U_A \approx 25\,\mathrm{eV}$ for deuteron target.[36)]

For the density of quasi-free mobile deuterons (or protons) in the reaction zone, ρ_i in eq. (14), we define a fractional number $f(E_b)$ as

$$\rho_i = f(E_b)\rho_{tm} \tag{19}$$

where ρ_{tm} is the density of target metal atoms, and E_b is the incident beam deuteron (or proton) laboratory kinetic energy. For the Ta and Pd metal targets, ρ_{tm} are 5.54×10^{22} and $6.80 \times 10^{22}\,\mathrm{cm}^{-3}$, respectively.

Comparisons of $F_{exp}(E)$ and $F_{theo}(E)$ are given below for D(d,p)T, ^{6}Li(d,α)^{4}He, and ^{6}Li(p,α)^{3}He reactions. Theoretical analysis for ^{7}Li(d,α)^{5}He[10)] and ^{7}Li(p,α)^{4}He[14)] reactions are expected to be similar to the ^{6}Li(d,α)^{4}He and ^{6}Li(p,α)^{3}He cases, respectively because of the isotopic independence of our theoretical formulation.

For the bare $S(E)$-factor, we have adopted the following expression,

$$S(E) = S(0) + S_1E + S_2E^2. \tag{20}$$

Values of the parameters $S(0)$, S_1, and S_2 in eq. (20) are shown in Table I.

4.1 D+D reactions

For the (D+D) reaction, we choose the deuteron beam experiment with TaD_x($x \approx 0.127$ corresponding to $Ta_{7.9}D$[8)]) target carried out by Raiola *et al.*[8)] In order to fit the experimental data represented by $R_{ij}^{exp}(E, U_e^{exp})$, eq. (15), we calculate R_{ij}, eq. (16) with one parameter ρ_i, the quasi-free deuteron density given by eq. (19). We have extracted $f(E_b)$ in eq. (19) by fitting R_{ij} to $R_{ij}^{exp}(E_bU_e^{exp})$, eq. (15). In eq. (14), we assume $\rho_c = \rho_i$. The extracted values of $f(E_b)$ are shown in Table II. As shown in Table II, $f(E_b)$ or ρ_i increases as E_b increases, which may be physically reasonable. We note that, at $E_b = 4\,\mathrm{keV}$, $\rho_i = f(E_b)\rho_{tm} \approx 2.55 \times 10^{16}\,\mathrm{cm}^{-3}$, and hence a reaction zone volume of $V_{int}(E_b) = 3.7 \times 10^{-5}\,\mathrm{cm}^3$ contains about one trillion quasi-free deuterons. Intersections of $F_{exp}(E) = F_{theo}(E)$ which is equivalent to $R_{ij} = R_{ij}^{exp}(E, U_e^{exp})$ are shown in Fig. 1 at $E = 4, 7$, and $10\,\mathrm{keV}$, corresponding to $f(E) = 4.6 \times 10^{-7}$, 3.1×10^{-6}, and 8.1×10^{-6}, respectively, as given in Table II. These extracted values of $f(E)$ for $\rho_i = f(E)\rho_{tm}$ [eq. (19)] satisfy the relation $f(4\,\mathrm{keV}) < f(7\,\mathrm{keV}) < f(10\,\mathrm{keV})$ or $\rho_i(4\,\mathrm{keV}) < \rho_i(7\,\mathrm{keV}) < \rho_i(10\,\mathrm{keV})$. This is physically consistent with expectations that the density of quasi-free mobile deuterons increases at higher temperatures (see p. 310 of ref. 27) in the target metal reaction zone, resulting from larger input power of higher energy deuteron beam incident on the reaction zone.

4.2 D+Li reactions

For the (D+Li) reactions, we carry out our theoretical analysis of the experimental data obtained by Kasagi *et al.*[10)] for ^{6}Li(d,α)^{4}He reaction with Pd^6Li_x ($x \approx 6\%$) target. In order to fit the experimental data represented by $R_{ij}^{exp}(E, U_e^{exp})$, eq. (15), we calculate R_{ij}, eq. (16) with one parameter ρ_i, the quasi-free deuteron density given by eq. (19). We have extracted $f(E_b)$ in eq. (19) by fitting R_{ij} to $R_{ij}^{exp}(E_bU_e^{exp})$, eq. (15). We assume $\rho_c = \rho_i$ in eq. (14). The extracted values of $f(E_b)$ are shown in Table III. As shown in Table III, $f(E_b)$ or ρ_i increases as E_b increases, which may be physically reasonable. Intersections of $F_{exp}(E) = F_{theo}(E)$ which is equivalent to $R_{ij} = R_{ij}^{exp}(E, U_e^{exp})$ are shown in Fig. 2 at $E = 30, 40$, and $60\,\mathrm{keV}$, corresponding to $f(E) = 5.8 \times 10^{-6}$, 2.0×10^{-5}, and 8.8×10^{-5}, respectively, as given in Table III. These extracted values of $f(E)$ for $\rho_i = f(E)\rho_{tm}$ [eq. (19)] satisfy the relation $f(30\,\mathrm{keV}) < f(40\,\mathrm{keV}) < f(60\,\mathrm{keV})$ or $\rho_i(30\,\mathrm{keV}) < \rho_i(40\,\mathrm{keV}) < \rho_i(60\,\mathrm{keV})$. This is physically consistent with expectations that the density of quasi-free mobile deuterons increases at higher temperatures (see p. 310 of ref. 27) in the target metal reaction zone, resulting from larger input power of higher energy deuteron beam incident on the reaction zone.

4.3 p+Li reactions

For the (p+Li) reactions, we investigate the experimental data for ^{6}Li(p,α)^{3}He reaction obtained by Cruz *et al.*[14)] from the proton beam experiments with Pd^6Li_x ($x = 1\%$) target. In order to fit the experimental data represented by $R_{ij}^{exp}(E, U_e^{exp})$, eq. (15), we calculate R_{ij}, eq. (16) with one parameter ρ_i, the quasi-free deuteron density given by eq. (19). We have extracted $f(E_b)$ in eq. (19) by fitting R_{ij} to $R_{ij}^{exp}(E_bU_e^{exp})$, eq. (15). In eq. (14) we assume $\rho_c = \rho_i$. The extracted values of $f(E_b)$ are shown in Table IV. As shown in Table IV, $f(E_b)$ or ρ_i increases as E_b increases, which may be physically reasonable. Intersections of $F_{exp}(E) =$

Table I. Parameters for the bare S-factor used in this paper.

Reaction	$S(0)$ (keV-b)	S_1 (barns)	S_2 (b/keV)
D(d,p)T[8)]	53	0.48	—
^{6}Li(d,α)^{4}He[37)]	16.9×10^3	−41.6	28.2×10^{-3}
^{6}Li(p,α)^{3}He[14)]	3.0×10^3	−3.02	1.93×10^{-3}

Table II. Values of $f(E_b)$, $\Delta x(E_b)$, $V_{int}(E_b)$, $V_{int}(E_b)R^Q_{ij}$, $R^{bt}_{ij}(E_b, U_A)$, and R_{ij} at different values of the beam deuteron laboratory kinetic energy E_b for the D(d,t)T reaction calculated from eqs. (19), (1b)–(3b), (1), (14), (10), and (16) respectively.

E_b (keV)	$f(E_b)$ eq. (19)	$\Delta x(E_b)$ (cm)	$V_{int}(E_b)$ (cm^3)	$V_{int}(E_b)R^Q_{ij}$ (s^{-1})	$R^{bt}_{ij}(E_b, U_A)$ (s^{-1})	R_{ij} (s^{-1})
4	4.6×10^{-7}	2.1×10^{-5}	3.7×10^{-5}	5.9×10^{-2}	1.7×10^{-2}	7.6×10^{-2}
7	3.1×10^{-6}	2.8×10^{-5}	4.9×10^{-5}	3.6	3.7	7.3
10	8.1×10^{-6}	3.3×10^{-5}	5.8×10^{-5}	2.9×10	5.6×10	8.5×10
20	3.1×10^{-5}	4.7×10^{-5}	8.2×10^{-5}	5.9×10^{2}	3.5×10^{3}	4.1×10^{3}
30	5.2×10^{-5}	5.7×10^{-5}	1.0×10^{-4}	2.1×10^{3}	2.2×10^{4}	2.4×10^{4}

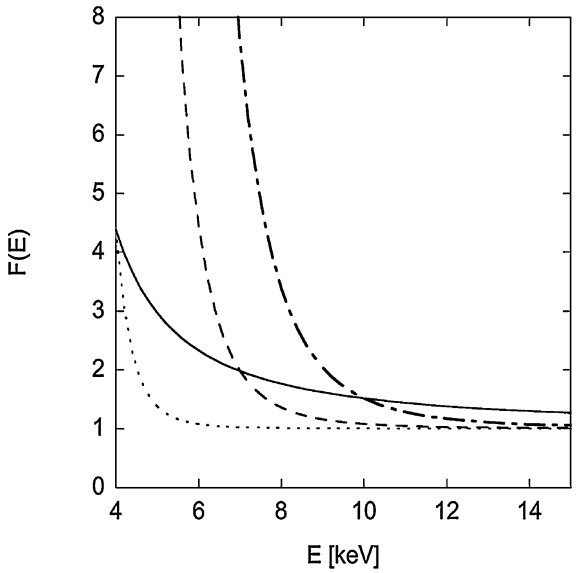

Fig. 1. Enhancement factors $F_{exp}(E)$ [eq. (17)] and $F_{theo}(E)$ [eq. (18)] for D(d,p)T reaction with Ta target as a function of the deuteron laboratory kinetic energy E. The solid line represents the parameterization of the experimental data $F_{exp}(E)$ calculated from eq. (17) with $U_e^{exp} = 309$ eV.[18] The dotted, dashed and dot-dashed lines represent our theoretical calculations of $F_{theo}(E)$ from eq. (18) with $U_A = 25$ eV, using the quasi-free deuteron densities specified by eq. (19) with $f(E) = 4.6 \times 10^{-7}$, 3.1×10^{-6}, and 8.1×10^{-6}, respectively, of the Ta density (5.54×10^{22} cm^{-3}).

$F_{theo}(E)$ which is equivalent to $R_{ij} = R^{exp}_{ij}(E, U^{exp}_e)$ are shown in Fig. 3 at $E = 30, 40,$ and 60 keV, corresponding to $f(E) = 1.9 \times 10^{-5}$, 4.1×10^{-5}, and 1.0×10^{-4}, respectively, as given in Table IV. These extracted values of $f(E)$ for $\rho_i = f(E)\rho_{tm}$ [eq. (19)] satisfy the relation $f(30\,keV) < f(40\,keV) < f(60\,keV)$ or $\rho_i(30\,keV) < \rho_i(40\,keV) < \rho_i(60$ keV).

This is physically consistent with expectations that the density of quasi-free mobile deuterons increases at higher temperatures (see p. 310 of ref. 27) in the target metal reaction zone, resulting from larger input power of higher energy deuteron beam incident on the reaction zone.

5. Discussion and Suggested Experimental Tests

Based on the theoretical formula for the QPNF rates given by eq. (14), we suggest several experimental tests. We note that R^Q_{ij}, eq. (14), depends on a product of three densities $\rho_c\rho_i\rho_j$ where ρ_i is the density of quasi-free mobile deuteron i (or proton) in the reaction zone, ρ_j is the density of stationary deuteron j (or Li) in the reaction-zone, and ρ_c is the density of charge scattering centers encountered by a quasi-free mobile deuteron i. If ρ_i, ρ_j, or ρ_c can be increased in the low-energy beam experiments, we expect that the observed reaction rates will increase. We note that the $\rho_c\rho_i\rho_j$ dependence for the QPNF rate is a new feature and differs from the $\rho_i\rho_j$ dependence for the conventional plasma nuclear fusion rate.

ρ_c can be either $\rho_c \approx \rho_i$ or $\rho_c \approx \rho_i + \rho_k$, where ρ_k can be the density of target nuclei (ρ_j), metal nuclei (ρ_{tm}) (such as Pd), or other impurity nuclei (ρ_{im}) (such as O in PdO target), or any combination of these three (ρ_j, ρ_{tm}, and ρ_{im}) in the reaction zone of the metal target. There is an indication of this prediction on ρ_c from recent deuteron beam experiments. Kasagi *et al.*[7] find that a PdO target produces a larger enhanced rate for the reaction D(d,p)T compared with Pd target, and Cruz *et al.*[14] find that a PdLi target produces larger enhanced rates for the reactions ^{7}Li(p,α)^{4}He and ^{6}Li(p,α)^{3}He, compared with a Li target. We suggest additional experimental tests of this type to be done in order to confirm this theoretical prediction.

Another interesting prediction from eq. (14) is that the reaction rate can be increased by increasing the density ρ_i of quasi-free mobile deuteron (or proton). For experimental tests of this prediction, we suggest two experimental tests during deuteron (or proton) beam experiments: (1) application of electric current (AC or DC with appropriate frequencies) to the target metal and (2) application of laser beam with appropriate frequencies on the reaction zone on the surface of the metal target.

Table III. Values of $f(E_b)$, $\Delta x(E_b)$, $V_{int}(E_b)$, $V_{int}(E_b)R^Q_{ij}$, $R^{bt}_{ij}(E_b, U_A)$, and R_{ij} at different values of the beam deuteron kinetic energy E_b for the ^{6}Li(d,α)^{4}He reaction calculated from eqs. (19), (1b)–(3b), (1), (14), (10), and (16), respectively.

E_b (keV)	$f(E_b)$ eq. (19)	$\Delta x(E_b)$ (cm)	$V_{int}(E_b)$ (cm^3)	$V_{int}(E_b)R^Q_{ij}$ (s^{-1})	$R^{bt}_{ij}(E_b, U_A)$ (s^{-1})	R_{ij} (s^{-1})
30	5.8×10^{-6}	4.3×10^{-5}	5.5×10^{-6}	0.1	0.1	0.2
40	2.0×10^{-5}	5.0×10^{-5}	6.3×10^{-6}	1.5	2.5	4.0
50	4.8×10^{-5}	5.7×10^{-5}	7.1×10^{-6}	9.2	2.3×10	3.2×10
60	8.8×10^{-5}	6.2×10^{-5}	7.8×10^{-6}	3.4×10	1.2×10^{2}	1.5×10^{2}
70	1.4×10^{-4}	6.8×10^{-5}	8.5×10^{-6}	9.5×10	4.1×10^{2}	5.1×10^{2}

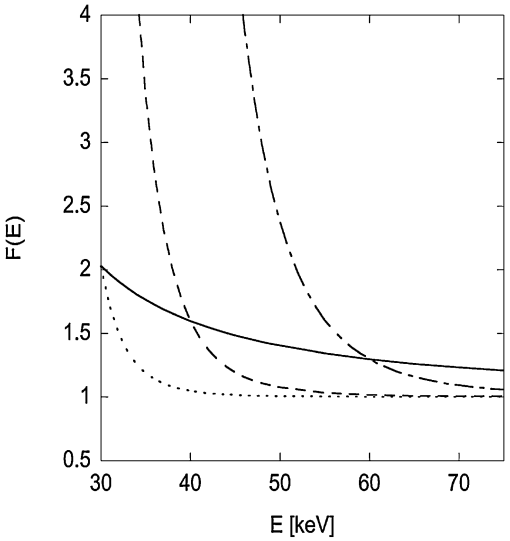

Fig. 2. Enhancement factors $F_{exp}(E)$ [eq. (17)] and $F_{theo}(E)$ [eq. (18)] for ^{6}Li(d,α)^{4}He reaction with Pd^{6}Li$_x$ ($x \approx 6\%$) target as a function of the deuteron laboratory kinetic energy E. The solid line represents the parameterization of the experimental data $F_{exp}(E)$ calculated from eq. (17) with $U_e^{exp} = 1500\,eV$.[10] The dotted, dashed and dot-dashed lines represent our theoretical calculations of $F_{theo}(E)$ using eq. (18) with $U_A = 175\,eV$, for $f(E) = 5.8 \times 10^{-6}$, 2.00×10^{-5}, and 8.8×10^{-5}, respectively, of the Pd density ($6.8 \times 10^{22}\,cm^{-3}$).

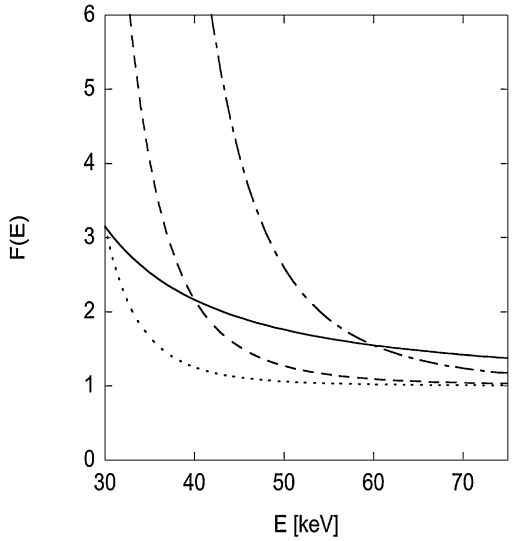

Fig. 3. Enhancement factors $F_{exp}(E)$ [eq. (17)] and $F_{theo}(E)$ [eq. (18)] for ^{6}Li(p,α)^{3}He reaction with Pd^{6}Li$_x$ ($x = 1\%$) target as a function of the deuteron laboratory kinetic energy E. The solid line represents the parameterization of the experimental data calculated from eq. (17) with $U_e^{exp} = 3760\,eV$.[14] The dotted, dashed and dot-dashed lines represent our theoretical calculations of $F_{theo}(E)$ using eq. (18) with $U_A = 175\,eV$, for $f(E) = 1.9 \times 10^{-5}$, 4.1×10^{-5}, and 1.0×10^{-4}, respectively, of the Pd density ($6.8 \times 10^{22}\,cm^{-3}$).

The suggested experiment (1) is based on experimental evidences[25,26,38–41] that the applied electric field in a metal causes protons (deuterons) in metal to become mobile, thus leading to a higher density for the quasi-free mobile protons (deuterons) in the reaction zone during proton (deuteron) beam experiments.

For the suggested experiment (2), it is anticipated that the incident laser will raise the temperature of the reaction zone and also increase the density of the quasi-free mobile protons (deuterons) in the reaction zone during proton (deuteron) beam experiments. We note that proton (deuterons) mobility takes various, temperature dependent forms, as illustrated in Fig. 6.2 of ref. 27. The mobility extends to "fluidlike" motion at temperatures comparable to the interstitial site or self-trapping, $\sim$0.15 eV binding energy. As stated in ref. 27, page 310, "In the highest-temperature region, H atoms no longer remain within the potential wells of interstitial sites but undergo free motion like the motion of atoms in gases." Therefore it is expected that this mobile fluid forms a heavy charged particle plasma[30] within the metal.

Since the reaction zone has a thin disk volume on the metal target surface, it is expected that the effect of the applied laser beam would be more effective in increasing reaction rates if it is incident nearly tangentially on the reaction-zone disk surface rather than incident nearly perpendicular to the reaction-zone disk surface. This prediction could be tested experimentally.

The target temperature dependence of the predicted reaction rates is to be investigated further in the future since N_A and ρ_i are expected to be temperature dependent. In eq. (14), ρ_i is expected to increase at higher temperatures (below the melting point), but may also decrease at higher temperatures since the deuteron (or proton) loading in the metal is expected to decrease.[25–27] Furthermore, the temperature in the reaction zone may not be the same as the target temperature.

6. Conclusions

We have investigated the effect of quantum corrections to the momentum distribution tail on the nuclear fusion reaction rates at low energies. Using the generalized momentum distribution function obtained Galitskii and Yakimets,[22] we have derived an approximate semi-analytical formula for nuclear fusion reaction rates. The approximate formula for this quantum plasma nuclear fusion

Table IV. Values of $f(E_b)$, $\Delta x(E_b)$, $V_{int}(E_b)$, $V_{int}(E_b)R_{ij}^Q$, $R_{ij}^{bt}(E_b, U_A)$, and R_{ij} at different values of the beam proton kinetic energy E_b for the ^{6}Li(p,α)^{3}He reaction calculated from eqs. (19), (1b)–(3b), (1), (14), (10), and (16), respectively.

E_b (keV)	$f(E_b)$ eq. (19)	$\Delta x(E_b)$ (cm)	$V_{int}(E_b)$ (cm^3)	$V_{int}(E_b)R_{ij}^Q$ (s^{-1})	$R_{ij}^{bt}(E_b, U_A)$ (s^{-1})	R_{ij} (s^{-1})
30	1.9×10^{-5}	3.1×10^{-5}	2.5×10^{-5}	1.4	0.7	2.1
40	4.1×10^{-5}	3.6×10^{-5}	2.7×10^{-5}	7.7	6.7	14.4
50	6.9×10^{-5}	4.1×10^{-5}	3.2×10^{-5}	2.5×10	3.2×10	5.7×10
60	1.0×10^{-4}	4.6×10^{-5}	3.6×10^{-5}	5.7×10	1.0×10^2	1.6×10^2
70	1.3×10^{-4}	5.0×10^{-5}	3.9×10^{-5}	1.1×10^2	2.6×10^2	3.7×10^2

(QPNF) rate is applied to theoretical analysis of anomalous enhancement of low-energy nuclear reaction rates observed from deuteron and proton beam experiments with metal targets. Comparison of our theoretical estimates with recent experimental data indicates that the theory may provide a reasonable and consistent theoretical explanation of the experimental data.

Based on our semi-analytical formula for the QPNF rates, we suggest a set of experiments for testing some of the predictions of our theoretical formula for the nuclear reaction rates.

1) S. Engstler, A. Krauss, K. Neldner, C. Rolfs, U. Schroder, and K. Langanke: Phys. Lett. B **202** (1988) 179.
2) U. Greife, F. Gorris, M. Junker, C. Rolfs, and D. Zahnow: Z. Phys. A **351** (1995) 107.
3) J. Kasagi, T. Murakami, T. Yajima, S. Kobayashi, and M. Ogawa: J. Phys. Soc. Jpn. **64** (1995) 3718.
4) H. Yuki, T. Satoh, T. Ohtsuki, T. Yorita, Y. Aoki, H. Yamazaki, and J. Kasagi: J. Phys. G **23** (1997) 1459.
5) H. Yuki, J. Kasagi, A. G. Lipson, T. Ohtsuki, T. Baba, T. Noda, B. F. Lyakhov, and N. Asami: JETP Lett. **68** (1998) 823.
6) K. Czerski, A. Huke, A. Biller, P. Heide, M. Hoeft, and G. Ruprecht: Europhys. Lett. **54** (2001) 449.
7) J. Kasagi, H. Yuki, T. Baba, T. Noda, T. Ohtsuki, and A. G. Lipson: J. Phys. Soc. Jpn. **71** (2002) 2881.
8) F. Raiola, P. Migliardi, G. Gyurky, M. Aliotta, A. Formicola, R. Bonetti, C. Broggini, L. Campajola, P. Corvisiero, H. Costantini, J. Cruz, A. D'Onofrio, Z. Fulop, G. Gervino, L. Gialanella, *et al.*: Eur. Phys. J. A **13** (2002) 377.
9) F. Raiola, P. Migliardi, L. Gang, C. Bonomo, G. Gyurky, R. Bonetti, C. Broggini, N. E. Christensen, P. Corvisiero, J. Cruz, A. D'Onofrio, Z. Fulop, G. Gervino, L. Gialanella, A. P. Jesus, *et al.*: Phys. Lett. B **547** (2002) 193.
10) J. Kasagi, H. Yuki, T. Baba, T. Noda, J. Taguchi, M. Shimokawa, and W. Galster: J. Phys. Soc. Jpn. **73** (2004) 608.
11) F. Raiola, L. Gang, C. Bonomo, G. Gyurky, M. Aliotta, H. W. Becker, R. Bonetti, C. Broggini, P. Corvisiero, A. D'Onofrio, Z. Fulop, G. Gervino, L. Gialanella, M. Junker, P. Prati, *et al.*: Eur. Phys. J. A **19** (2004) 283.
12) C. Rolfs for LUNA Collaboration: Prog. Theor. Phys. Suppl. No. 154 (2004) 373.
13) F. Raiola, B. Burchard, Z. Fulop, G. Gyurky, S. Zeng, J. Cruz, A. DiLeva, B. Limata, M. Fonseca, H. Luis, M. Aliotta, H. W. Becker, C. Broggini, A. D'Onofrio, L. Gialanella, *et al.*: J. Phys. G **31** (2005) 1141.
14) J. Cruz, Z. Fulop, G. Gyurky, F. Raiola, A. DiLeva, B. Limata, M. Fonseca, H. Luis, D. Schurmann, M. Aliotta, H. W. Becker, A. P. Jesus, K. U. Kettner, J. P. Ribeiro, C. Rolfs, *et al.*: Phys. Lett. B **624** (2005) 181.
15) H. J. Assenbaum, K. Langanke, and C. Rolfs: Z. Phys. A **327** (1987) 461.
16) Y. E. Kim: Fusion Technol. **19** (1991) 588.
17) C. Bonomo, G. Fiorentini, Z. Fulop, L. Gang, G. Gyurky, K. Langanke, F. Raiola, C. Rolfs, E. Somorjai, F. Streider, J. Winter, and M. Aliotta: Nucl. Phys. A **719** (2003) C37.
18) J. D. Jackson: *Classical Electrodynamics* (Wiley, New York, 1975) 2nd ed., pp. 496–497.
19) M. Coraddu, M. Lissia, G. Mezzorani, and P. Quarati: Eur. Phys. J. B **50** (2006) 11.
20) M. Coraddu, M. Lissia, G. Mezzorani, Y. V. Petrushevich, P. Quarati, and A. N. Starostin: Physica A **340** (2004) 490.
21) M. Coraddu, G. Mezzorani, Y. V. Petrushevich, P. Quarati, and A. Starostin: Physica A **340** (2004) 496.
22) V. M. Galitskii and V. V. Yakimets: Zh. Eksp. Teor. **51** (1966) 957 [Sov. Phys. JETP **24** (1967) 637].
23) Y. E. Kim and A. L. Zubarev: Jpn. J. Appl. Phys. **45** (2006) L552.
24) H. H. Anderson and J. F. Ziegler: *Hydrogen Stopping Powers and Ranges in All Elements* (Pergamon, New York, 1977).
25) F. A. Lewis: Platinum Met. Rev. **26** (1982) 74.
26) Q. M. Barer: *Diffusion in and through Solids* (Cambridge University Press, New York, 1941).
27) Y. Fukai: *The Metal–Hydrogen System* (Springer, New York, 2005) 2nd ed.
28) J. Kasagi: Proc. Int. Conf. Surface Modification Materials by Ion Beams, 2005, to be published in Surf. Coat. Technol.
29) P. Kalman and T. Keszthelyi: Nucl. Instrum. Methods Phys. Res., Sect. B **240** (2005) 781.
30) National Research Coun.: *Plasma Science* (National Academy Press, Washington, D.C., 1995), p. 1.
31) V. A. Belyakov: Sov. Phys. JETP **13** (1961) 850.
32) A. A. Abrikovsov, L. P. Gorkov, and I. E. Dzyaloshinski: *Methods of Quantum Field Theory in Statistical Physics* (Dover Publication, New York, 1963) pp. 36–42.
33) N. N. Bogoliubov: J. Phys. USSR **11** (1947) 23.
34) L. Pitaevskii and S. Stringari: *Bose-Einstein Condensation* (Clarendon Press, Oxford, 2003) Chap. 4, pp. 26–37.
35) Y. E. Kim, R. S. Rice, and G. S. Chulick: Mod. Phys. Lett. **6** (1991) 929.
36) L. Bracci, G. Fiorentini, V. S. Melezhik, G. Mezzorani, and P. Quarati: Nucl. Phys. A **513** (1990) 316.
37) A. Musumara, R. G. Pizzone, S. Blagus, M. Bogovac, P. Figueral, M. Lattuada, M. Milin, D. Miljanic, M. G. Pellegriti, D. Rendic, C. Rolfs, N. Soic, C. Spitaleri, S. Typel, H. H. Wolter, *et al.*: Phys. Rev. C **64** (2001) 068801.
38) A. Coehn: Z. Electrochem. **35** (1929) 676.
39) A. Coehn and W. Specht: Z. Phys. **83** (1930) 1.
40) B. Duhm: Z. Phys. **94** (1935) 34.
41) J. F. Mareche, J.-C. Rat, and A. Herold: J. Chim. Phys. Phys. Chim. Biol. **73** (1976) 983.